least-squares fitted straight lines for each of the solutes. The correlation coefficients indicate a fairly good linear relationship between ln D_{AB} and $1/T$. Examination of the ΔE values shows that, for the straight chain phenones, the "activation" energy decreases as the chain length increases. This can conceivably yield the contribution of a CH_2 group to the "activation" energy. Figure 7 shows a plot of ΔE vs. the carbon number of the alkane side chain. The general features of Figure 7 are very similar to those shown in Figure 5, and the discussion made regarding the latter figure might hold true here. To the advocate of the rate approach, the data in Table VII and Figure 7 indicate that on the average, each CH_2 group contributes initially about 73 cal to the "activation" energy, and that the contribution decreases as N increases. Ertl and Dullien[36] reported a linear relationship between "activation" energy and the log of the carbon number in the case of self-diffusion of some liquids, provided the carbon number is large enough. Such was not the case in the present study.

The similarities between Figures 5 and 7 are noteworthy. Although at this point we cannot offer any explanations, we feel that the resemblance is more than a coincidence. At this point, additional data are needed, especially at low temperatures where the fluidity approach should deviate from the picture given here. In addition, to take full advantage of the more rigorous hard sphere theories, data at a given temperature but at varying pressures should be gathered. This will help in adjusting the model for large nonspherical molecules diffusing in mixtures.

References and Notes

(1) A. Einstein, "Investigation on the Theory of the Brownian Movement", Dover Publication, New York, N.Y., 1956.
(2) S. Glasstone, K. J. Laidler, and H. E. Eyring, "The Theory of Rate Processes", McGraw-Hill, New York, N.Y., 1941.
(3) S. A. Rice and J. G. Kirkwood, *J. Chem. Phys.*, **31**, 901 (1954).
(4) R. K. Ghai, H. Ertl, and F. A. L. Dullien, *AIChE J.* **19**, 881 (1973); **20**, 1 (1974).
(5) A. J. Batschinski, *Z. Phys. Chem. (Leipzig)*, **84**, 643 (1913).
(6) J. H. Hildebrand, *Science*, **174**, 490 (1971).
(7) J. H. Hildebrand and R. H. Lamoreaux, *Proc. Nat. Acad. Sci. U.S.A.*, **71**, 3321 (1974).
(8) H. Ertl and F. A. L. Dullien, *J. Phys. Chem.*, **77**, 3007 (1973).
(9) B. J. Alder, W. E. Alley, and J. H. Dymond, *J. Chem. Phys.*, **61**, 1415 (1974).
(10) D. Chandler, *J. Chem. Phys.*, **62**, 1358 (1975).
(11) J. H. Dymond, *J. Chem. Phys.*, **60**, 969 (1974).
(12) J. DeZwaan and J. Jonas, *J. Chem. Phys.*, **62**, 4036 (1975).
(13) R. B. Bird, W. E. Stewart, and E. N. Lightfoot, "Transport Phenomena", Wiley, New York, N.Y., 1960.
(14) G. I. Taylor, *Proc. R. Soc. London, Ser. A*, **219**, 186 (1953).
(15) G. I. Taylor, *Proc. R. Soc. London, Ser. A*, **225**, 473 (1954).
(16) A. C. Ouano, *Ind. Eng. Chem. Fundam.*, **11**, 268 (1972).
(17) K. C. Pratt and W. A. Wakeham, *Proc. R. Soc. London, Ser. A*, **336**, 393 (1974).
(18) E. Grushka and E. J. Kikta, Jr., *J. Phys. Chem.*, **78**, 2297 (1974).
(19) H. Komiyama and J. M. Smith, *J. Chem. Eng. Data*, **19**, 384 (1974).
(20) P. F. Jhaveri, R. N. Trivedi, and K. Vasudera, *Diffus. Solutes Solution Fiber Syst., Proc. Symp.* (1973); *Chem. Abstr.*, **81**, 68883 (1974).
(21) A. C. Ouano and J. A. Carothers, *J. Phys. Chem.*, submitted for publication.
(22) B. J. Alder and J. H. Hildebrand, *Ind. Eng. Chem., Fundam.*, **12**, 387 (1973).
(23) H. T. Cullinan, Jr., and G. Kosanovich, *AIChE J.*, **21**, 195 (1975).
(24) J. C. Shieh and P. A. Lyons, *J. Phys. Chem.*, **73**, 3258 (1969).
(25) S. Nir and W. A. Stein, *J. Chem. Phys.*, **55**, 1598 (1971).
(26) H. Y. Lo, *J. Chem. Eng. Data*, **19**, 236 (1974).
(27) S. A. Sanni, C. J. D. Fell, and P. Hutchison, *J. Chem. Eng. Data*, **16**, 424 (1971).
(28) W. F. Calus and M. T. Tyn, *J. Chem. Eng. Data*, **18**, 377 (1973).
(29) L. R. Wilke and P. Chang, *AIChE J.*, **1**, 264 (1955).
(30) A. Couper and R. F. T. Stepto, *Trans. Faraday. Soc.*, **65**, 2486 (1969).
(31) R. D. Burkhart and J. C. Merrill, *J. Chem. Phys.*, **46**, 4985 (1967).
(32) D. V. S. Jain and K. K. Tewari, *Chem. Phys. Lett.*, **10**, 487 (1971).
(33) J. G. Kirkwood and J. Riseman, *J. Chem. Phys.*, **16**, 1565 (1948).
(34) C. J. Vadovic and C. P. Colver, *AIChE J.*, **19**, 546 (1973).
(35) A. L. Van Geet and A. W. Adamson, *J. Phys. Chem.*, **68**, 238 (1964).
(36) H. Ertl and F. A. L. Dullien, *AIChE J.*, **19**, 1215 (1973).

All-Electron Nonempirical Calculations of Potential Surfaces. III. Dissociation of Ketene into CH_2 and CO

Phil Pendergast and William H. Fink*

Contribution from the Department of Chemistry, University of California, Davis, California 95616.

Received February 13, 1975

Abstract: Ab initio calculations on the lower lying states of ketene have been performed using excited-state SCF and CI methods. The ground-state and first excited-state surfaces were searched so as to nearly find the optimum theoretical molecular geometry. Dissociations along both linear and bent paths departing from these geometries were then examined. The excited-state assignments of ketene and its controversial photochemistry are discussed in light of the calculated molecular orbital correlation diagrams, the SCF energies, the configuration interaction energies, and the weights of the configurations.

A qualitative and semiquantitative understanding of photochemical processes should be possible by quantum chemical calculations of the potential-energy surfaces involved in these processes. The present work is a state of the art application of quantum chemical methods to the primary photochemical decomposition reactions of ketene ($H_2C{=}C{=}O$). While the reliability of SCF methods of calculation for closed-shell, ground-state molecules in the vicinity of the equilibrium internuclear geometry is reasonably well understood, the situation is less clear for open-shell, excited-state molecules or for geometries far from the ground-state equilibrium. In certain situations, the inadequacy of the valence-shell atomic orbitals to describe low-lying Rydberg levels has become apparent;[1] in other situations, the states are simply not adequately described by a single-determinant wave function;[2] this latter difficulty often becomes particularly acute at asymptotic values of intermolecular distances where the imposition of a particular occupation precludes the SCF wave function from dissociating to the correct molecular or atomic fragments. The present work includes both an extended basis set and limited configuration interaction calculation in order to be reasonably sure of avoiding these possible deficiencies of a valence-shell SCF calculation. There remains considerable controversy over

*Author to whom correspondence should be addressed.

Table I. Experimental Values of Vertical Excitation Energies[a]

λ_{max}[b]	Excitation energy[c]	Assignment[d]
370	3.35[e]	$^3A_2(^3\Sigma_u^-)$ and $^3B_2(^3\Sigma_u^+)$
323	3.84	$^1A_2(^1\Sigma_u^-)$
213	5.82	$^1B_2(^1\Delta_u)$
170	7.29[f]	$^1B_2(^1\Sigma_u^+)$
155	8.00[f]	$^1B_2(^1\pi_g)$

[a] Reference 7 except as noted. [b] Nanometers. [c] Electron volts. [d] The term symbols in parentheses refer to the states of linear CO_2 with which these states would have correlated. [e] Reference 5. [f] Reference 9.

Table II. Calculated Values of Vertical Excitation Energies[a]

Excited configuration	SCF[b]	CI[b]
$^3A_2$	2.96	4.00
$^1A_2$	3.16	4.27
$^3B_1$	7.95	9.42
$^1B_1$	8.15	9.71
$^1A_1$		12.00

[a] Electron volts. [b] Results obtained at ground state theoretically optimized geometry.

the photochemistry of ketene both with respect to the assignment of its spectrum[3-9] and with respect to the photolysis.[10] An attempt to contribute to the resolution of these controversies and to contribute to the development and testing of quantum chemical methods motivated the calculations reported here.

Techniques

The calculations were carried out within the framework of performing a limited configuration interaction in an expansion set composed of the molecular orbitals obtained from an SCF calculation of the lowest lying state of a given irreducible representation. The basis set employed was the Gaussian lobe basis.[11,12] This was augmented by an approximate oxygen 3s orbital.[1] The closed-shell SCF calculations were performed in the conventional Hartree-Fock-Roothaan[13] manner as in previous work on formaldehyde photochemical reaction surfaces.[2] However, the open-shell SCF calculations were treated differently from the earlier work by employing a variant of the orthogonally constrained method of Segal[14] which had been originally programmed by J. L. Whitten and J. A. Horsley. The routine was revised by the present authors to increase its applicability and to adapt it to the Burroughs B6700 computer. All SCF results reported have been checked to verify that an inadvertent local minimum in the atomic orbital function space has been avoided. This checking required some care in the regions of the potential surface where changes in electronic configuration were occurring, but did not constitute a major difficulty in the work. Searches for the minimum-energy geometry were carried out on both the ground-state surface and the first excited state. The R_{CC} and R_{CO} internuclear distances and the OCC angle were systematically varied for both states. The configuration interaction calculations were performed using two separate programs. The four-index transformation program has been reported elsewhere.[15] The output integral list from this program was then interfaced with the configuration interaction program used in the previous work.[2] All changes required in this latter program were checked by verifying exact agreement (to within the numerical precision of the B6700 48-bit word) with results obtained from the earlier version. While a complete examination of the potential surface for all degrees of freedom would be desirable, compromises in the interest of economy of both human and machine costs must be made. It was decided to examine two different least motion dissociation paths—a linear C_{2v} dissociation departing from the lowest energy geometry of the calculated ground-state SCF point and a bent C_s dissociation departing from the lowest energy geometry of the calculated first excited state point.

Molecular Energies

Although it is difficult to establish useful estimates of error limits on calculated energy values, some feeling for the reliability of the generated surfaces may be obtained by comparing calculated quantities with their experimentally determined equivalents. Further comparisons with other calculations permit an assessment of the relative reliability of the present work among the hierarchy of available approaches.

The available experimental data with which comparison is possible are excitation energies of ketene and methylene and thermochemical differences between the heats of formation of ketene and of methylene and carbon monoxide. Table I lists the experimental values of apparent Franck-Condon maxima as reported by Rabalais et al.[7] along with the tentative assignments made by them to the upper electronic state of these bands. It must be remarked that the maximum reported by them as observed by Dixon and Kirby[5] at 370 nm is regarded as a continuation of the band peaking at 323 nm by Laufer and Keller[8] because of the similarities of the vibrational spacings and the apparent smooth dependence of the extinction coefficient on wave length throughout this region. These latter authors deferred assignment of the bands until reliable, detailed molecular orbital calculations were available.

The calculated vertical excitation energies obtained with the SCF and CI wave functions are reported in Table II along with the nominal or dominant electronic configuration of the calculated state. Ignoring the assignments for the moment, there is reasonable agreement between the experimental and the calculated excitation energy patterns. There are two states with excitation energies around 3-4 eV above the ground state and then an appreciable energy gap (experimentally about 2 eV, theoretically about 5 eV) before the appearance of a cluster of several states. There is essential agreement in the assignment of the lower energy band (bands) to the transition associated with the $^{1,3}A_2$ states of ketene. The assignments of Table I[7] were based upon correlations with the lower excited states of CO_2 and upon extended Hückel calculations of CO_2, H_2CCO, and H_2CNN. Unfortunately Table I of ref 7 upon which the correlations were based, although correct for the correlation of CO_2 from $D_{\infty h}$ to C_{2v} by bending the OCO angle (one of the C_2 axes perpendicular to the C_∞ axis of $D_{\infty h}$ becomes the principal C_2 axis of C_{2v}), does not apply for ketene and diazomethane (the C_∞ axis of $D_{\infty h}$ becomes the principal C_2 axis of C_{2v}). The important difference in correlation which applies in this latter case is $\{\pi_{u,g} \rightarrow b_1 + b_2\}$ not $\{(\pi_u \rightarrow a_1 + b_1), (\pi_g \rightarrow a_2 + b_2)\}$. Consequently the designations of the molecular orbitals and electronic states used for ketene and diazomethane in ref 7 are not the conventional Schoenflies notation and do not correspond with the present results and notation. For the important states of usual near-uv photolysis of ketene then the calculated excitation energies are in reasonable semiquantitative (±1 eV) agreement with the experimental spectrum.

Although no careful optimization of methylene and carbon monoxide geometries was attempted, the asymptotic values of the calculated potential surfaces may be compared with energies of carbon monoxide and methylene. The results obtained from the bent dissociation path at R_{CC} = 10.0 are compared with the experimental quantities in Table III. $\Delta E°$ refers to the reaction

Table III. Experimental and Calculated Energies[a] Related to Methylene

	Exptl	CI
ΔE°	81[b]	27[b]
$^3B_1 - {}^1B_1$	<0.99	1.42
$^1A_1 - {}^1B_1$	0.88	0.68

[a] Electron volts except where noted. [b] In kcal/mol.

$$OCCH_2 \rightarrow OC + CH_2$$

No attempt to account for the difference between the bottoms of the wells (calculated values) and the zero point energies (experimental values) has been made. The experimental value is obtained from compendium tabulations of ΔH_f°.[16,17] There is a great deal of uncertainty in the experimental singlet–triplet splitting energy for methylene and a recent paper by Carr[18] presents some evidence for a very low value of 1.4 kcal/mol for this splitting. We prefer the older estimates for reasons discussed below. The well-established experimental excitation energy between the two lowest methylene singlets is well represented by the calculations. The thermochemical energy differences are not, but quantitative calculations of such severe electronic changes normally require more extensive treatment of correlation energy than is attempted here and consequently the poor value obtained is not surprising. It is in the proper sense and of the correct order of magnitude.

Several previous calculations on ketene have been reported which enable comparison with other methods of electronic structure calculation. Letcher, Unland, and van Wazer,[19] using a (73/73/3) uncontracted basis set of 1s and 2p Gaussian functions, have reported a number of one-electron properties; the total energy of their wave function was −151.5077. The present approach calculated at the same geometry gives −151.4790. The present SCF result at the experimental ground-state geometry[20] is −151.4799. Basch,[21] using a 36-G basis set, obtained a SCF energy of −151.6721 at the geometry of Moore and Pimentel.[22] This latter calculation employs a basis set nearly double that of the present work. The judicious loss of 0.2 au in the total energy compared with the most extensive calculation reported is not severe in view of the greater geometric exploration possible with the reduced basis size. The lowest energy for the CI calculations on the ground state obtained in the present work is −151.5679 which is to be compared with the six-configuration MC-SCF[21] result of −151.6967. In summary, although the present work has not obtained as low a total energy as the best previously reported results, the compromises made in basis-set flexibility are compensated by the ability to perform a significant number of calculations at various geometries.

Results and Discussion

Table IV presents the results of SCF calculations which led to the partial optimization of the ground-state and first excited-state geometries of ketene for the R_{CC} and R_{CO} internuclear distances and the in-plane OCC internuclear angle (R_{CH} = 1.071 Å and HCH angle = 122° 35′ were held constant at all times). The minimum energy calculated for the ground state was at R_{CC} = 1.31 Å, R_{CO} = 1.23 Å, and OCC angle = 180°. The minimum energy calculated for the first excited triplet state was at R_{CC} = 1.59 Å, R_{CO} = 1.35 Å, and OCC angle = 138°. A similar geometry optimization by Del Bene[23] using a minimal STO-3G basis yielded ground-state minimum-energy parameters of R_{CC} = 1.30 Å, R_{CO} = 1.18 Å, OCC angle = 180°, and excited-state parameters of R_{CC} = 1.36 Å, R_{CO} = 1.26 Å, OCC angle = 127°. These are to be compared with the experimental values for the ground state[20] of R_{CC} = 1.315, R_{CO} = 1.16, and R_{CH} = 1.075 Å and HCH angle = 122°. There is substantial agreement among the minimal STO-3G results, the present work, and the experimental values for the ground state. There is qualitative agreement only between the STO-3G results and the present work for the excited-state geometry, in that increased bond lengths, especially R_{CC}, and an in-plane bend are found in the excited state. The present work also finds the excited-state and ground-state surfaces to lie in closer proximity than did the minimal STO-3G calculation as the adiabatic excitation energy ($^3A'' \leftarrow {}^1A_1$) was found to be 2.46 eV vs. 0.81 eV in the results reported here.

Table IV. Geometric Variation of SCF Energies

			$-E - 151$[c]	
R_{CC}[a]	R_{CO}[a]	∠CCO[b]	X	$^3A_2(^3A'')$
2.30	2.50	180	0.4598	0.3604
2.20	2.80	180	0.3830	0.3330
2.75	2.25	180	0.4905	0.4216
3.00	2.50	180	0.4662	0.4372
2.25	3.25	180	0.3407	0.3274
2.75	2.75	180	0.4614	0.4078
2.48	3.02	180	0.4191	0.3832
2.48	2.52	180	0.4924	0.4042
2.48	2.32	180	0.4967	0.3954
2.48	2.19	180	0.4799	0.3711
2.48	2.52	160	0.4854	0.4163
2.48	2.52	150	0.4764	0.4259
2.48	2.66	169	0.4732	0.4050
3.00	2.33	180	0.4712	0.4361
2.40	2.33	180	0.4867	0.3766
4.00	2.40	180	0.3528	0.3517
2.48	2.65	150	0.4636	0.4242
2.48	2.65	140	0.4525	0.4322
2.48	2.65	130	0.4372	0.4360
2.48	2.80	150	0.4433	0.4212
2.48	2.80	140	0.4345	0.4300
2.48	2.80	130	0.4220	0.4342
2.48	2.40	150	0.4802	0.4236
2.48	2.40	140	0.4651	0.4306
2.48	2.40	130	0.4454	0.4331
2.60	2.55	148.7	0.4789	0.4421
2.60	2.56	138.4	0.4652	0.4489
2.60	2.71	138.4	0.4505	0.4393
2.60	2.70	148.8	0.4624	0.4320
2.48	2.52	140	0.4633	0.4333
2.48	2.52	130	0.4245	0.4194
2.48	2.65	135	0.4455	0.4348
2.48	2.65	125	0.4276	0.4356
2.48	2.80	135	0.4288	0.4328
3.00	2.56	138.4	0.4366	0.4668

[a] Distances in bohrs. [b] Angles in degrees. [c] Energy in hartrees.

Starting from the geometry of the minimum-energy calculation for the ground state, a linear least-motion dissociation path to the products CH_2 and CO was calculated. A similar bent-least-motion dissociation path to the same products was followed from the calculated minimum-energy geometry of the $^3A''$ state; the separation along the linear pathway proceeded maintaining the geometrical parameters of each fragment fixed at their original values and maintaining C_{2v} symmetry as the R_{CC} distance was increased. The bent pathway similarly maintained the original geometrical parameters of the fragments fixed while the methylene was pulled away from the carbon monoxide such that the line bisecting the HCH angle always intersected the carbon monoxide axis at the same point with an angle of 138.4°.

Figure 1 displays the molecular orbital one-electron energies calculated for the linear dissociation pathway. The calculated points are shown as small solid circles imbedded in the line connecting energies of corresponding molecular or-

Table V. Molecular Orbital Occupations

	C_{2v}							C_s						
Ketene	$2b_2$	$1b_2$	$7a_1$	$1b_1$	$2b_1$	$8a_1$	$3b_1$	7a′	8a′	9a′	1a″	2a″	10a′	3a″
$CO + CH_2$	$1b_2$	1π	5σ	1π	2π	$3a_1$	$1b_1$	$1b_2$	1π	5σ	1π	2π	$3a_1$	$1b_1$
I	2	2	2	2	2	0	0	2	2	2	2	2	0	0
II	2	2	2	2	0	2	0	2	2	2	2	0	2	0
III	2	2	2	2	1	0	1	2	2	2	2	1	0	1
IV	2	2	2	2	0	0	2	2	2	2	2	0	0	2
V	2	2	2	2	0	1	1	2	2	2	2	0	1	1

bitals. The curves are labeled on the left with molecular orbital designations for the C_{2v} point group.[24] The orbitals of ground-state ketene are occupied through the $2b_1$ orbital. These orbitals correlating with carbon monoxide are connected with dashed lines to the appropriately labeled point on the extreme right. Those not so connected correlate to orbitals of methylene with the same C_{2v} irreducible representation. The ketene $7a_1$ orbital correlates to the carbon monoxide 5σ orbital, while the ketene $1b_1$ and $1b_2$ orbitals become the degenerate carbon monoxide 1π orbitals. The $2b_1$ and $3b_2$ orbitals of ketene correlate to the carbon monoxide 2π orbital and $9a_1$ to 6σ. Particularly noteworthy is the precipitous drop in energy of the $8a_1$ orbital between 4 and 5 bohrs while the $2b_1$ orbital undergoes an equally dramatic rise in energy. The magnitude of the changes is of course exaggerated because of the change in occupation which occurs at this value of R_{CC}. Careful examination of the curves, however, will show that there is an a_1 orbital rapidly descending in energy as one moves to larger values of R_{CC} which starts as the $9a_1$ orbital off scale on the left, produces an avoided crossing between $9a_1$ and $8a_1$ at about 4 bohrs, becomes the occupied $8a_1$ at 5 bohrs and eventually correlates with the $3a_1$ orbital of methylene. It is because of this rapid change in energy and subsequent change in molecular orbital occupation that the ground-state potential-energy surface is able to correlate with the lowest singlet state of methylene $^1A_1$. Table V summarizes the molecular orbital occupations: the first row gives the ketene designations; and the second gives the CO or CH_2 orbital to which these correlate. Configuration I is the ground-state occupation of ketene; configuration II is the configuration which takes over at R_{CC} = 5 bohrs; configuration V correlates with the accepted ground-state configuration for methylene and carbon monoxide; configurations III and IV will be discussed below. As is apparent from the second row of the table, the ground-state ketene occupation would dissociate to an ionic configuration of CH_2^{2+} and CO_2^{2-} without the change in occupation.

The correlation diagram for the bent dissociation has not been presented because of its morphology similar to that for the linear dissociation. The only differences arise because both a_1 and b_2 irreducible representations transform as a′ under C_s symmetry with the result that more avoided crossings separate the two clusters of orbital energies involving $1b_2$ through $2b_2$ and the higher virtual orbitals $3b_2$, $3b_1$, and $9a_1$. Also in the bent geometry, the change in molecular orbital occupation occurs between 3 and 4 bohrs rather than between 4 and 5. The important molecular orbital occupations are summarized in the right-half of Table V, where the second row again gives the orbitals of CO and CH_2 to which the ketene orbitals correlate. Each row designates the same configuration under both C_{2v} and C_s point groups.

The SCF programs used in this investigation permit the rigorous determination of upper bounds for the lowest singlet and triplet states of each irreducible representation of the molecular point group. The data obtained for the linear dissociation are displayed in Figure 2 for the lower states of

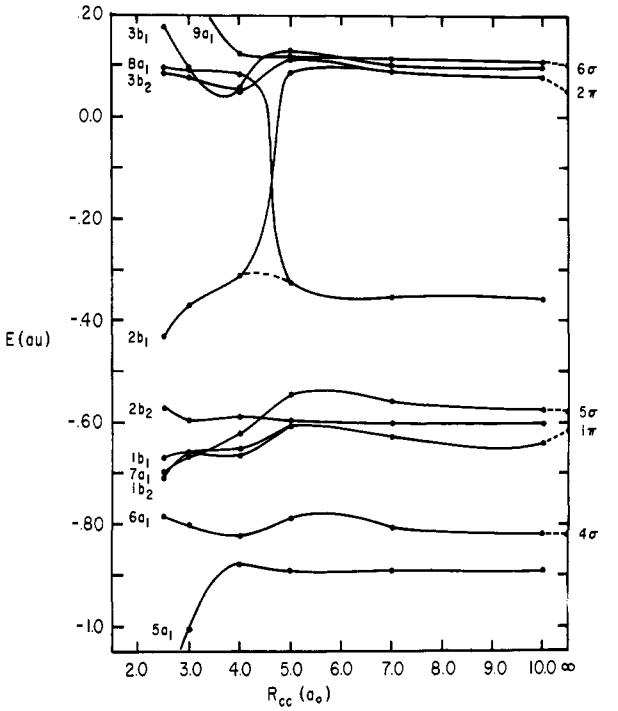

Figure 1. Molecular orbital correlation diagram. The one-electron energies of the molecular orbitals for ground-state ketene are plotted as a function of the OC–CH_2 distance. Labels on the left are the ketene orbitals. Those which correlate to CO orbitals are connected with dashed lines to a point labeled with the CO orbital designation. Those not so connected correlate to methylene orbitals of the same irreducible representation label as the ketene. Only the orbitals with negative one-electron energies are occupied.

ketene. The ground state $^1A_1$ has the configuration I of Table V which has asymptotic limits of $CO_2^{2-}(^1\pi)$, $CH_2^{2+}(^1A_1)$, until R_{CC} = 5 bohrs, where it takes on configuration II with asymptotes $CO_2(^1\Sigma^+)$, $CH_2(^1A_1)$. The $^3A_1$ state has configuration III of Table V, which has asymptotic limits of $CO_2^-(^2\pi)$, $CH_2^+(^2B_1)$; the $^{1,3}A_2$ states are obtained by the promotion $2b_1 \rightarrow 3b_2$ from configuration I, and the $^{1,3}B_1$ states are obtained by the promotion $2b_1 \rightarrow 8a_1$ from configuration I. $^{1,3}B_2$ states could be derived from configuration I by the double promotion $(2b_1)^2 \rightarrow (8a_1)^1(3b_2)^1$. These states have not been examined in the present work since, being double excitations of the ketene ground configuration, they are expected to lie higher than the configurations examined. The $^{1,3}A_2$ states have only been followed to R_{CC} = 4.0 bohrs because with no change in occupation these states will dissociate to $CH_2^+ + CO_2^-$ as may be determined from the correlation diagram in Figure 1. More will be said about the $^3A_1$ state when discussing the configuration interaction results below. The minimal STO-3G calculations also found this state to be low lying in the SCF approximation.[23] The $^3B_1$ state correlates properly to the ground states of CH_2 and CO, the $^1B_1$ state to the second excited state of CH_2 and ground state CO, while the ketene ground-state surface after change of occupation at

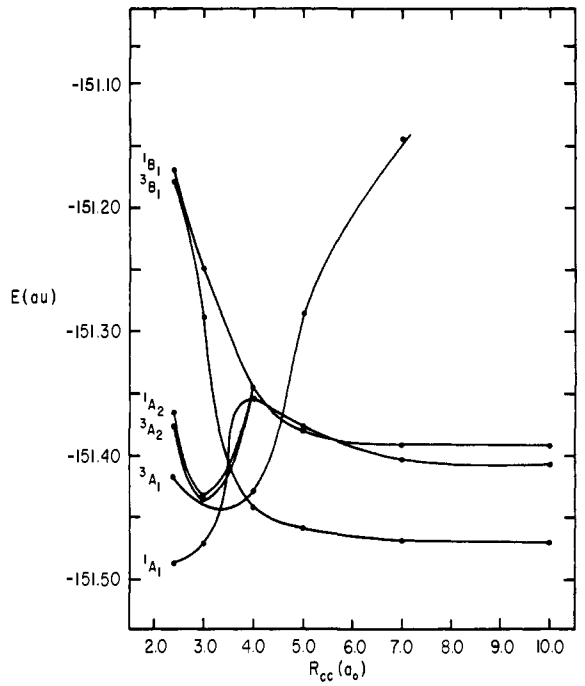

Figure 2. SCF calculated energies for the linear dissociation of ketene.

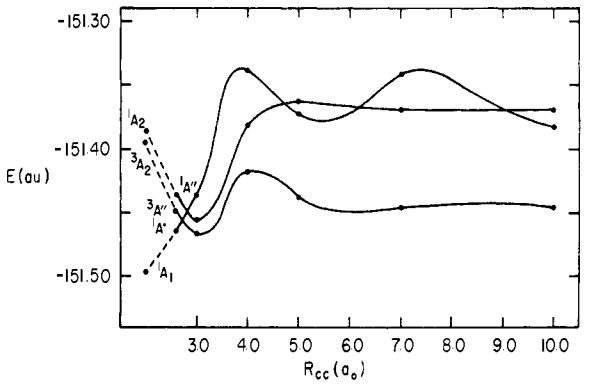

Figure 3. SCF calculated energies for the bent dissociation of ketene. The leftmost points connected with dashed lines provide a visual comparison of the energy of the C_{2v} states of the molecule with which the solid curves connect. The curves are labeled with both the C_{2v} designations and the C_s designations.

R_{CC} = 5 bohrs correlates correctly to the $^1A_1$ state of CH_2 and ground state CO.

Figure 3 presents the SCF results for the bent dissociation pathway. The points on the extreme left are the energies obtained for the labeled states at the geometry found for the ground state. These are connected to the bent geometry surfaces to which they correspond with dashed lines. As both A_2 and B_1 irreducible representations of C_{2v} transform as A″ under C_s, the $^3A_2$ and $^3B_1$ surfaces do not cross in the bent geometry but merge into the curve displayed for $^3A''$. Similarly the corresponding singlets $^1A_2$ and $^1B_1$ merge into the curve displayed for $^1A''$. The calculated points are indicated by solid circles imbedded in the solid line connecting them.

Unlike many molecular dissociation processes, the dissociation of ketene into CH_2 and CO is correctly represented by the SCF-MO approximation for the lower states of the molecule. The ground state of ketene is accommodated by a change in occupation of the molecule between 4 and 5 bohrs. The first excited open-shell singlet state can correlate to the correct asymptote along the bent path because the lowest singlet state of methylene is an open-shell singlet and because the A_2 and B_1 irreducible representations both transform under A″. Similarly the first excited open-shell triplet can obtain the correct asymptote along the bent path because the ground state of methylene is the triplet and because of the coalescence of the A_2 and B_1 irreducible representations into A″. Figures 2 and 3 then are very reasonable qualitative representations of the potential surfaces important for photolytic processes in ketene. However, there were a few disquieting features of these curves which necessitated a somewhat more thorough consideration of effects beyond the SCF-MO approximation. The low-lying triplet A_1 state of Figure 2 and the apparent minimum in the $^1A'$ surface at about 5 bohrs are perhaps the two most outstanding. Further, if the important qualitative features of the SCF curves are retained in a modest treatment of correlation effects, then it may be reasonably expected that these features will also remain in the true molecular potential surface.

The choice of configurations to be included in the CI calculations was limited so as not to exceed 100 Slater determinants. All CI calculations were performed in the expansion set of molecular orbitals obtained for the lowest state of that irreducible representation. For the excited states, only doubly excited configurations of the type $(\varphi_i)^2 \rightarrow (\varphi_k)^2$ were considered using only the first seven virtual orbitals and only the six highest doubly occupied orbitals. Table VI gives the configurations used in the ground-state CI calculations expressed as excitations from configuration I of Table V. Excitations involving the seven highest occupied molecular orbitals to the first six virtuals are shown. Since numerous configurations among this set of occupied and virtual orbitals are possible, truncation to the set of configurations shown was achieved by a series of preliminary CI calculations at the geometry of the ground-state minimum SCF energy retaining only those with weighting coefficients exceeding 10^{-3} in the ground-state vector.

Table VI. Configurations Used in Ground-State CI Calculations

1.	I	19.	$1b_1^2 \rightarrow 8a_1^2$
2.	$2b_1^2 \rightarrow 2b_1 3b_1$	20.	$1b_1^2 \rightarrow 3b_2 4b_2$
3.	$2b_1^2 \rightarrow 3b_2^2$	21.	$1b_1^2 2b_2^2 \rightarrow 1b_1 2b_2 3b_2 3b_1$
4.	$2b_1^2 \rightarrow 8a_1 9a_1$	22.	$1b_2^2 \rightarrow 3b_2^2$
5.	$2b_1^2 \rightarrow 8a_1^2$	23.	$1b_2^2 \rightarrow 8a_1^2$
6.	$2b_1^2 \rightarrow 3b_1^2$	24.	$1b_2^2 \rightarrow 3b_1^2$
7.	$2b_1^2 \rightarrow 9a_1^2$	25.	$1b_2^2 \rightarrow 10a_1^2$
8.	$2b_1^2 \rightarrow 4b_2^2$	26.	$1b_2^2 \rightarrow 4b_2^2$
9.	$2b_2^2 2b_1^2 \rightarrow 2b_2 2b_1 3b_2 3b_1$	27.	$7a_1^2 \rightarrow 3b_2^2$
10.	$2b_2^2 2b_1^2 \rightarrow 2b_2 2b_1 3b_1 4b_2$	28.	$7a_1^2 \rightarrow 3b_1^2$
11.	$2b_2^2 \rightarrow 3b_2^2$	29.	$7a_1^2 \rightarrow 9a_1^2$
12.	$2b_2^2 \rightarrow 8a_1^2$	30.	$6a_1^2 \rightarrow 3b_2^2$
13.	$2b_2^2 \rightarrow 3b_1^2$	31.	$6a_1^2 \rightarrow 3b_1^2$
14.	$2b_2^2 \rightarrow 9a_1^2$	32.	$6a_1^2 \rightarrow 9a_1^2$
15.	$2b_2^2 \rightarrow 4b_2^2$	33.	$6a_1^2 \rightarrow 10a_1^2$
16.	$2b_2^2 \rightarrow 3b_2 4b_2$	34.	$5a_1^2 \rightarrow 9a_1^2$
17.	$1b_1^2 \rightarrow 3b_2^2$	35.	$5a_1^2 \rightarrow 10a_1^2$
18.	$1b_1^2 \rightarrow 3b_1^2$	36.	$5a_1^2 \rightarrow 9a_1 10a_1$

The results of the CI calculations for the linear and bent dissociations are displayed in Figures 4 and 5, respectively. Only those roots of the CI hamiltonian matrices which fell below −151.10 au for some part of the pathway are displayed. Calculated points are shown as solid circles imbedded in the lines connecting them. The curves are labeled on the left with the appropriate state of ketene and on the right with the state of methylene to which they correlate. The energies of the states at the ground-state geometry are plotted in the figure and connected to the appropriate state with a dashed line. Several features about the curves must be mentioned. Although the solid lines connecting the calculated points are believed to represent the trends in the data, it is clear from the number of solid circles in the figures that a considerable amount of interpretation regarding the loca-

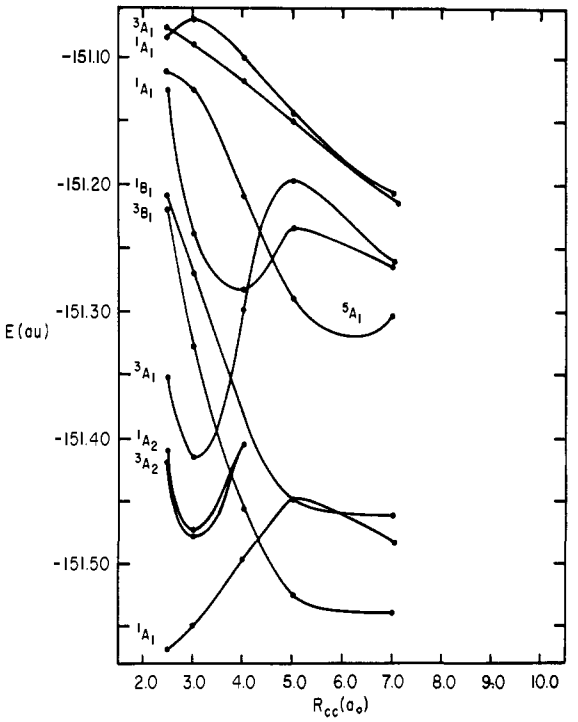

Figure 4. CI calculated energies for the linear dissociation. Only those roots of the CI hamiltonian which came below −151.10 hartrees for some value of the R_{CC} distance are plotted.

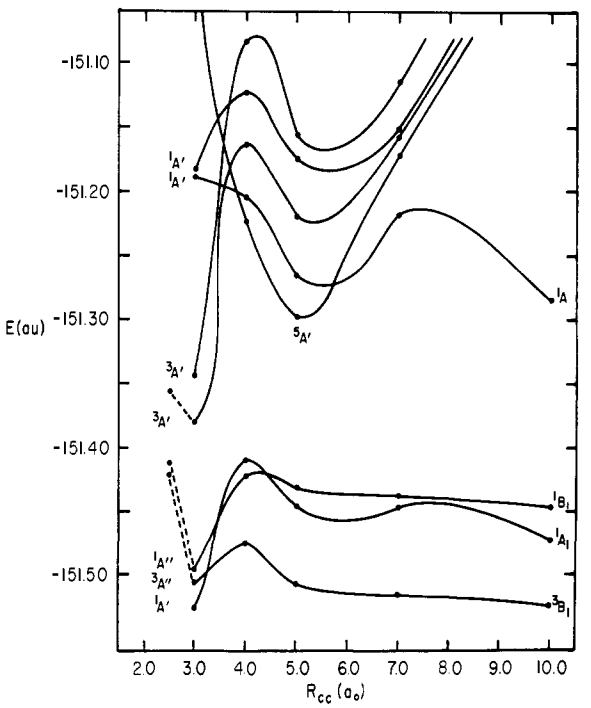

Figure 5. CI calculated energies for the bent dissociation of ketene. The leftmost points connected to the solid curves with dashed lines provide a visual comparison of the energy of the C_{2v} states of the molecule with which these surfaces connect.

tions of these curves between calculated points was required. Consequently although the rough form of the surfaces is established, no succinct location of maxima or minima is possible. The asymptotic limits of the curves on the right all correspond to some state of methylene and the ground Σ^+ state of carbon monoxide. While the figures bear the term symbol of the appropriate methylene state on the right, the corresponding term symbol for carbon monoxide is suppressed. The qualitative similarity of the lower energy curves of Figure 4 and the MCSCF results of Basch[21] for the linear dissociation is striking. There are some interesting avoided crossings in the singlet manifold of states which can be identified in the CI results. The more complete data are available for the bent dissociation and, in Figure 5, a $^1A'$ state which begins in the lower left corner and rises toward the upper right corner crosses two $^1A'$ states which start in the upper left corner and drop toward the lower right. Avoided crossing produces the maximum in the ketene ground state $^1A'$ and a minimum in the second $^1A'$ state at 4–5 bohrs. A second avoided crossing is experienced by the second $^1A'$ state which produces the apparent maximum in this state between 7 and 8 bohrs. Secondary effects of singlet interactions in this region may produce the maximum depicted for the ground state also. If so, the minimum thereby produced in this state at about 6 bohrs may be significant and may be indicating the existence of a relatively stable geometry in some related molecular distortion such as the oxirene intermediate postulated by Rowland et al.[10,25] to account for their results of ^{14}C exchange from $^{14}CH_2$ to ^{14}CO.

These changes in character of the lowest two singlet roots of the A′ CI may be further explored by examination of the contributions of the major components to the CI wave function. Table VII presents a selection of the major components of the first and second singlet roots as the R_{CC} distance increases. The configurations of these components are as given in Table V, the Roman numerals corresponding with the occupation given there. The change in character from I to II of the ground state between 3 and 4 bohrs has

Table VII. Weights of Major Components in the Bent CI Dissociation

	3.0	4.0	5.0	7.0	10.0
			Lowest $^1A'$		
I	0.9355	0.0703	0.1225	−0.0006	0.0000
II	−0.0047	−0.9660	−0.9610	−0.9392	0.9506
III	−0.0424				
IV	−0.2425	0.0283	0.0019	0.1430	−0.1828
			Second $^1A'$		
I	−0.1637	−0.9472	0.8845	0.0075	0.0000
II	−0.3414	−0.0608	0.1294	−0.1286	0.1706
III	−0.5613				
IV	−0.2986	0.2165	−0.2299	−0.9814	0.9802

been discussed as being the change which enables the ground-state surface of ketene to dissociate to the lowest energy $^1A_1$ state of methylene. The expected first excited singlet state of ketene, configuration III, is the dominant configuration of the state at R_{CC} = 3.0 but, even this close to the ground-state ketene geometry, has very significant contributions from other configurations. By 4 bohrs, the configuration which was formerly ground-state ketene has now almost completely taken over the first excited singlet surface. At 5 bohrs it remains dominant, but configuration IV, the double excitation $(2b_1)^2 \rightarrow (3b_1)^2$ from ketene ground state, has begun to be significant; at R_{CC} = 7.0, it has taken over the representation of the surface. From the second row of Table V, it is clear that configuration IV has asymptotic limits of $CO(^1\Sigma^+)$ and $^1A_1$* doubly excited methylene. The interaction of this state with the ground-state surface at 7 and 10 bohrs is evident by the 0.1 weight of configuration IV in the ground-state CI vector. This latter configurational weight in the ground-state CI vector lends credence to the interpretations of the lower singlet root energies discussed above.

The presence of a low-lying quintet root in both the linear and bent dissociations with a minimum at about 5–7 bohrs, although well above the usual photolytic energies employed, may lead to interesting phosphorescent effects at higher

energies with the possibility of unusually strong spin interactions. The quintet is a member of the jumble of states accessible to ketene at higher energies which provide numerous possibilities for decay channels.

Focusing attention on the three lowest energy surfaces which are involved in the usual photolyses of ketene, there is very little change between the CI and SCF calculated surfaces as is apparent when comparing Figures 2 and 4 and Figures 3 and 5. The SCF approximation in this particular case is capable of a semiquantitatively correct representation of the surfaces from the vicinity of ground-state ketene all the way to dissociated CH_2 + CO. This is unusual for molecular processes involving bond rupture and comes about because the ground state of methylene is a triplet. Consequently the closed-shell singlet molecular orbital configuration for ground-state ketene is capable of correctly representing the dissociation of that state to the excited closed-shell singlet state of methylene. To do so, a change in orbital occupation must occur, but the SCF wave function can easily accommodate that change in description of molecular electronic structure. The open-shell singlet and triplet configurations are then quite capable of representing their respective dissociations to the corresponding states of methylene. There is an appreciable difference between the SCF and CI results in the relative placement of the lowest $^3A_1$ surface, the SCF results placing it below the $^{1,3}A_2$ surfaces while the CI results place it above them. It is possible that, because the configurations were chosen to maximally lower the ground-state energy, the lowest triplet state emerging from the resultant CI is held at a higher energy than it would be if the CI had been chosen to improve its energy as well. However countering this argument is that, in the SCF calculations, the $^3A_1$ state would be expected to lie lower relative to the ground state because of the so-called Fermi correlations between the parallel spins and, to balance this, additional treatment of the Coulomb correlations for the ground state are required. The placement of this state must remain in doubt.

Ketene Photochemistry

The electronic spectrum of ketene was first studied by Lardy,[3] and the photochemical production of ethylene and carbon monoxide was initially reported by Norrish, Crone, and Saltmarsh.[4] The photodissociation mechanism was suggested to consist of the following reactions:[26]

$$CH_2CO + h\nu \rightarrow CH_2 + CO \quad \text{(I)}$$

$$CH_2 + CH_2CO \rightarrow C_2H_4 + CO \quad \text{(II)}$$

$$CH_2CO + h\nu \rightarrow {}^*CH_2CO_m \quad \text{(III)}$$

$${}^*CH_2CO_m \rightarrow CH_2 + CO \quad \text{(IV)}$$

$${}^*CH_2CO_m \rightarrow CH_2CO \quad \text{(V)}$$

$${}^*CH_2CO_m + CH_2CO \rightarrow 2CH_2CO \quad \text{(VI)}$$

$^*CH_2CO_m$ represents an electronically and vibrationally excited ketone molecule. The reactions

$$CH_2 + CH_2CO \rightarrow C_2H_4CO \quad \text{(VII)}$$

$$CH_2CO + xCH_2CO \rightarrow CO + \text{polymer} \quad \text{(VIII)}$$

were proposed[26,27] to explain CO quantum yields in excess of 2 from short-wave-length (<270 nm) irradiation, where the ratio of CO yield to C_2H_4 yield is 2.2. The present work bears directly only on the essentially unimolecular processes in this mechanism, reactions I, III, IV, and V, and can only make arguments of inference about intermolecular processes.

Ketene photolysis at 365 nm gave low quantum yields which was interpreted as being caused by collisional deactivation and internal conversion of electronically excited ketene molecules.[28] A subsequent study[29] found that increased ketene pressure decreased the quantum yield. Such pressure dependence was taken to indicate that the excited state is long-lived as compared with the mean time between collisions.

Considerable evidence that triplet as well as singlet methylene is formed during the photolysis is available. That triplet dominance can be inferred at the longest wave lengths used in the photolyses is taken as evidence that triplet ketene must be the precursor of triplet methylene.[30,31] The ratio of triplet to singlet methylene produced at various photolysis wave lengths as determined by the stereospecificity of methylene addition to double bonds has been summarized by Calvert and Pitts.[32] However, the observation of ketene (triplet 2.65 eV above ground state) quenching of biacetyl emission[6] (triplet 2.39 eV above ground state) implies that triplet ketene is either not a long-lived intermediate state of the photolysis[32] or that the triplet state of ketene lies closer to the ground state than does that of biacetyl. The placement of the ketene triplet state at 2.65 eV above the ground state is based on the upper limit to the lower dissociation energy given by Dixon and Kirby.[5] As this was an upper limit estimate and as the assignment itself has been questioned,[8] it is difficult to accept the quenching of biacetyl emission by ketene as conclusive evidence for the absence of a ketene triplet intermediate state.

Although the calculations reported here can not resolve the controversies in ketene photochemistry, it is worthwhile to see to what extent they are consistent with existing interpretations of photochemical mechanisms and what possible additional interpretations they may suggest. The energies of the calculated vertically excited states have been included in Figures 4 and 5 to assist in providing an approximate visual impression of the energy immediately available for the primary photo processes. A ketene molecule vertically excited to the $^1A_2$ state of Figure 4 appears to have nearly enough energy to dissociate directly on its own surface along the bent dissociation pathway, the curve labeled $^1A''$ in Figure 5. It could collisionally deactivate to the $^1A'$ surface anywhere along the dissociation pathway and would have greatest probability of doing so at those values of R_{CC} where these surfaces appear to come into closest proximity. The resultant singlet methylene could collisionally deactivate to the triplet. If the spin-orbit terms of the hamiltonian, which have been neglected in these calculations, are large enough to produce significant contamination of the singlet with triplet, the vertically excited molecule would appear to have more than ample energy to overcome the much smaller energy barrier along the $^3A''$ pathway. The frequency of this event would of course be limited by the small amount of such contamination which is likely, but this would be a possible means for singlet ketene to be precursor to triplet methylene. Alternatively if the vertically excited molecule were collisionally deactivated to a lower lying vibrational level on its own $^1A''$ surface, intersystem crossing would be more probable and there does appear to be the possibility of a long-lived triplet existing in a well, as shown in Figure 5, with the molecule bent at the central carbon. The calculated curves would then be consistent with both singlet and triplet ketene as precursor to the triplet methylene. A somewhat bizarre and highly speculative alternative to both of these is suggested by the near coincidence of the $^1A_2$ and $^3A_2$ surfaces in Figure 4 at R_{CC} = 4.0. Such close proximity of the surface would suggest relatively efficient intersystem crossing in this region of the potential surface. If, because of the large difference in geometry be-

tween the minimum-energy $^1A''$ state and the ground state $^1A_1$, a resulting low Franck-Condon overlap would make the $^1A''$ state relatively long-lived and, if the energy of this state were so low as to preclude dissociation to $^1A_1$ methylene, the photolytic process most energetically possible would be to $^3B_1$ methylene. Further, such dissociations, although uncommon and therefore with anticipated low quantum yield, could be collisionally activated to the linear geometry where intersystem crossing might proceed more efficiently. Although certainly not investigated in the range of molecular geometries considered here, such a long-lived bent intermediate might also find an accessible pathway to an oxirene-like geometry on the ground-state surface. This speculation could be immediately dismissed if the methylene $^3B_1$-$^1A_1$ splitting could be established as being as low as 1-2 kcal/mol[18,33] since such a small energy difference could be easily overcome from available thermal energies. Because of the discrepancy between this value for the singlet-triplet splitting in methylene and the best available theoretical, computational estimates of 10-20 kcal/mol,[34,35,36] it is worthwhile to recall the methods of estimation which resulted in the lower value. By observing the product ratio of $[C_2H_6]/[n\text{-}C_4H_{10}]$ as a function of total pressure formed in mixtures of ketene-NO-CH_4 and C_3H_8 photolyzed with 313-nm light at low percentage conversion, assuming a mechanism, applying steady state conditions, assigning an overall scale factor to the product ratio plot, assuming RRKM theory, and fitting the theoretical curve to their plot, Halberstadt and McNesby[33] were able to extract a value for the quantity $\langle\epsilon^+\rangle$, the energy of the excited complex above the critical value required for reaction at absolute zero. This quantity, along with known thermochemical quantities and a 2-kcal/mol estimate of available thermal energy, leaves 2.5 kcal/mol which can be interpreted as the methylene singlet-triplet splitting energy. In the more recent report,[18] the product analysis of ketene photolysis at 350 nm yielded an estimate of singlet methylene production as 13 ± 2%. Argument that a low quantum yield and a high pressure dependence would suggest thermal equilibration of the intermediate methylenes justified the assumption of a Boltzmann distribution for them. Conversion of the 13% singlet to an energy difference between singlet and triplet in a Boltzmann distribution led Carr[18] to the value 1.4 kcal/mol for the singlet-triplet splitting. While both of these reports are very sophisticated and ingenious utilizations of available data to obtain an estimate for a quantity which is difficult to determine, because of their extensive utilization of theoretical interpretation they can not be considered as direct experimental determination of the singlet-triplet splitting.

Conclusion

Reported here are the results of SCF and CI calculations undertaken to examine the energy related properties of the lower lying states of ketene. Partial optimization of the molecular geometric parameters were carried out for the SCF surfaces for the ground and first excited singlet state surfaces. Reasonable agreement with experimental values for the ground-state molecular geometry, ketene excitation energies, methylene excitation energies, and thermochemical values of ketene dissociation have been obtained. Both linear and bent least-motion dissociation pathways have been examined and the resulting curves discussed with respect to the inferences which can be made about the photochemical dissociation of ketene into carbon monoxide and methylene. The changes in electronic structure during the course of dissociation have been discussed with the aid of the calculated SCF one-electron energies and the weighting coefficients for the dominant components in the configuration interaction. Substantial agreement with previous SCF and MCSCF results were obtained along the linear dissociation pathway. No previous results along the bent pathway were available. A $^3A_1$ state found low lying in the SCF approximation was found to be raised to significantly higher energy in the CI calculations. The calculated curves were found to be consistent with either singlet ketene or triplet ketene as a precursor to triplet methylene. An unusual interpretation of a long-lived intermediate was suggested by the calculated curves which could conceivably accommodate the existing, apparently conflicting evidence regarding the long-wavelength formation of triplet methylene, but its highly speculative nature at this time must be stressed.

Acknowledgments. The extensive computations required for the results reported here were made possible by the support of the UC Davis Computer Center. Much of this support in the early stages of the work was derived from NSF Grant GJ-462 awarded through the NSF Office of Computing Activities.

References and Notes

(1) J. A. Horsley and W. H. Fink, *J. Chem. Phys.*, **50**, 750 (1969).
(2) W. H. Fink, *J. Am. Chem. Soc.*, **94**, 1073, 1078 (1972).
(3) G. C. Lardy, *J. Chim Phys. Phys.-Chim. Biol.*, **21**, 353 (1924).
(4) R. G. W. Norrish, H. G. Crone, and O. Saltmarsh, *J. Chem. Soc.*, 1533 (1933).
(5) R. N. Dixon and G. H. Kirby, *Trans. Faraday Soc.*, **62**, 1406 (1966).
(6) M. Grossman, G. P. Semeluk, and I. Unger, *Can. J. Chem.*, **47**, 3079 (1969).
(7) J. W. Rabalais, J. M. Mcdonald, V. Scherr, and S. P. McGlynn, *Chem. Rev.*, **71**, 73 (1971).
(8) A. H. Laufer and R. A. Keller, *J. Am. Chem. Soc.*, **93**, 61 (1971).
(9) W. C. Price, J. P. Teegan, and A. D. Walsh, *J. Chem. Soc.*, 920 (1951).
(10) One of the more recent contributions to the area is: D. C. Montague and F. S. Rowland, *J. Am. Chem. Soc.*, **93**, 5381 (1971); other contributions are cited in detail below.
(11) J. L. Whitten, *J. Chem. Phys.*, **39**, 349 (1963).
(12) J. L. Whitten, *J. Chem. Phys.*, **44**, 359 (1966).
(13) C. C. J. Roothaan, *Rev. Mod. Phys.*, **23**, 69 (1951).
(14) G. A. Segal, *J. Chem. Phys.*, **53**, 360 (1970).
(15) P. Pendergast and W. H. Fink, *J. Comput. Phys.*, **14**, 286 (1974).
(16) "JANAF Thermochemical Tables", 2nd ed, D. R. Stull and H. Prophet, project directors, National Bureau of Standards, U.S. Government Printing Office, Washington, D.C., 1971.
(17) "Selected Values of Chemical Thermodynamic Properties", Circular of the National Bureau of Standards 500, U.S. Government Printing Office, Washington, D.C., 1952.
(18) R. W. Carr, *J. Chem. Phys.*, **53**, 4716 (1970).
(19) J. N. Letcher, M. L. Unland, and J. R. van Wazer, *J. Chem. Phys.*, **50**, 2185 (1969). There is an error in the reported geometry of this calculation. In private communication, the authors have reported that an error in the value of the cosine used to hand calculate the atomic coordinates resulted in the calculation actually having been performed at the geometry $R_{CH} = 1.063$ Å, $\angle HCH = 124°7'$.
(20) H. R. Johnson and M. W. P. Strandberg, *J. Chem. Phys.*, **20**, 687 (1952).
(21) H. Basch, *Theor. Chim. Acta*, **28**, 151 (1973).
(22) C. B. Moore and G. C. Pimentel, *J. Chem. Phys.*, **38**, 2816 (1963).
(23) J. Del Bene, *J. Am. Chem. Soc.*, **94**, 3713 (1972).
(24) The molecule is oriented with z axis along the molecular axis and lying in the yz plane according to the usual convention: *J. Chem. Phys.*, **23**, 1997 (1955). Thus x transforms as b_1. The orientation used by Basch (ref 21) results in the interchange of the usual designations b_1 and b_2.
(25) R. L. Russell and F. S. Rowland, *J. Am. Chem. Soc.*, **92**, 7508 (1970).
(26) A. N. Strachan and W. A. Noyes, Jr., *J. Am. Chem. Soc.*, **76**, 3258 (1954).
(27) G. B. Kistiakowsky and W. L. Marshall, *J. Am. Chem. Soc.*, **74**, 88 (1952).
(28) G. B. Porter, *J. Am. Chem. Soc.*, **79**, 1878 (1957).
(29) B. T. Connelly and G. B. Porter, *Can. J. Chem.*, **36**, 1640 (1958).
(30) A. N. Strachan and D. E. Thornton, *J. Phys. Chem.*, **70**, 952 (1966).
(31) A. N. Strachan and D. E. Thornton, *Can. J. Chem.*, **46**, 2353 (1968).
(32) J. G. Calvert and J. N. Pitts, "Photochemistry", Wiley, New York, N.Y., 1966, pp 391-392.
(33) M. L. Halberstadt and J. R. McNesby, *J. Am. Chem. Soc.*, **89**, 3417 (1967).
(34) S. V. O'Neil, H. F. Schaefer, III, and C. F. Bender, *J. Chem. Phys.*, **55**, 162 (1971).
(35) J. F. Harrison and L. C. Allen, *J. Am. Chem. Soc.*, **91**, 807 (1969).
(36) J. M. Foster and S. F. Boys, *Rev. Mod. Phys.*, **32**, 305 (1960).